Excitatory Mechanisms in the Suprachiasmatic Nucleus: The Role of AMPA/KA Glutamate Receptors

STEPHAN MICHEL,* JASON ITRI,* AND CHRISTOPHER S. COLWELL
Mental Retardation Research Center, Department of Psychiatry and Biobehavioral Sciences, University of California, Los Angeles, California 90024-1759

Michel, Stephan, Jason Itri, and Christopher S. Colwell. Excitatory mechanisms in the suprachiasmatic nucleus: the role of AMPA/KA glutamate receptors. *J Neurophysiol* 88: 817–828, 2002; 10.1152/jn.00023.2002. A variety of evidence suggests that the effects of light on the mammalian circadian system are mediated by direct retinal ganglion cell projection to the suprachiasmatic nucleus (SCN). This synaptic connection is glutamatergic and the release of glutamate is detected by both N-methyl-D-asparate (NMDA) and amino-methyl proprionic acid/kainate (AMPA/KA) iontotropic glutamate receptors (GluRs). It is well established that NMDA GluRs play a critical role in mediating the effects of light on the circadian system; however, the role of AMPA/KA GluRs has received less attention. In the present study, we sought to better understand the contribution of AMPA/KA-mediated currents in the circadian system based in the SCN. First, whole cell patch-clamp electrophysiological techniques were utilized to measure spontaneous excitatory postsynaptic currents (sEPSCs) from SCN neurons. These currents were widespread in the SCN and not just restricted to the retino-recipient region. The sEPSC frequency and amplitude did not vary with the daily cycle. Similarly, currents evoked by the exogenous application of AMPA onto SCN neurons were widespread within the SCN and did not exhibit a diurnal rhythm in their magnitude. Fluorometric techniques were utilized to estimate AMPA-induced calcium (Ca^{2+}) concentration changes in SCN neurons. The resulting data indicate that AMPA-evoked Ca^{2+} transients were widespread in the SCN and that there was a daily rhythm in the magnitude of AMPA-induced Ca^{2+} transients that peaked during the night. By itself, blocking AMPA/KA GluRs with a receptor blocker decreased the spontaneous firing of some SCN neurons as well as reduced resting Ca^{2+} levels, suggesting tonic glutamatergic excitation. Finally, immunohistochemical techniques were used to describe expression of the AMPA-preferring GluR subunits GluR1 and GluR2/3s within the SCN. Overall, our data suggest that glutamatergic synaptic transmission mediated by AMPA/KA GluRs play an important role throughout the SCN synaptic circuitry.

INTRODUCTION

The circadian clock regulates many aspects of an organism's behavior and physiology. In mammals, the part of the nervous system responsible for most circadian behavior can be localized to a pair of structures in the hypothalamus known as the suprachiasmatic nucleus (SCN). Importantly, when SCN cells are removed from the organism and maintained in a brain slice preparation, they continue to generate circadian rhythms in

electrical activity, secretion, and gene expression (reviewed by Gillette 1997). Previous studies suggest that the basic mechanism responsible for the generation of these rhythms is intrinsic to individual cells in the SCN (Welsh et al. 1995) and perhaps in other cell types (Balsalobre et al. 1998). The core molecular mechanism driving these cellular oscillations appears to be a negative feedback loop operating at the transcriptional/translational levels (e.g., King and Takahashi 2000; Reppert and Weaver 2001). The circadian oscillator located in these cells generates a rhythm that repeats with a frequency of close to but not equal to 24 h. To function adaptively, these cells must be synchronized to the exact 24 h cycle of the physical world. The daily cycle of light and dark is the dominant cue used by organisms to synchronize their biological clocks to the environment. Thus a major goal of research in this area is to understand the mechanisms by which light acts to synchronize circadian oscillators.

The SCN receives photic information directly through a monosynaptic projection from the retina known as the retinal hypothalamic tract (RHT) as well as through an indirect connection from the intergeniculate leaflet (Ibata et al. 1999; Moore 1996; Morin 1994). The RHT appears to be necessary and sufficient for entrainment by light, and thus a focal point of research in this area has been to identify the transmitters released by the RHT and the resulting signal transduction cascades activated in the SCN. There is now very good evidence that glutamate mediates the effects of light on the circadian system through its role as a transmitter at the RHT/SCN synaptic connection (Colwell and Menaker 1996; Ebling 1996; Mintz et al. 1999; Obrietan et al. 1998). In the simplest case, light causes the release of glutamate that initiates a signal-transduction cascade in SCN neurons that ultimately results in a phase shift of the circadian system. This release of glutamate is detected by both N-methyl-D-asparate (NMDA) and amino-methyl proprionic acid/kainate (AMPA/KA) iontotropic glutamate receptors (GluRs). There is a variety of evidence to suggest that the NMDA receptor plays a special role in the transduction of the light input to the SCN and that the function of these receptors is gated by the circadian system (e.g., Colwell 2001; Pennartz et al. 2001; for review: Ebling 1996). The role of AMPA/KA-type GluRs in the SCN is less clear. The receptors are present in the SCN (e.g., Gannon and Rea 1993,

---

* The first two authors contributed equally to this study.
Address for reprint requests: C. S. Colwell, Mental Retardation Res. Ctr., University of California, 760 Westwood Plaza, Los Angeles, CA 90024-1759 (E-mail: ccolwell@mednet.ucla.edu).

1994; Mikkelsen et al. 1995; Stamp et al. 1997; van den Pol et al. 1994) and a circadian rhythm of AMPA receptor GluR2/3 subunit immunoreactivity has been reported (Chambille 1999). The excitatory postsynaptic responses recorded in the SCN are largely mediated by AMPA/KA GluRs (e.g., Cahill and Menaker 1989; Cui and Dyball 1996; de Vries et al. 1994; Jiang et al. 1997; Kim and Dudek 1991). Finally, light-induced phase shifts of the circadian rhythm in locomotor activity were prevented by the administration of AMPA/KA GluR blockers (Colwell and Menaker 1992; Rea et al. 1993). In many synapses, NMDA GluRs work in concert with the AMPA/KA GluRs that are responsible for the initial depolarization of the postsynaptic membrane. The depolarization is required before the membrane potential moves into the voltage range at which the NMDA GluR can become active. Postsynaptic responses of SCN neurons seem to follow the same principal with an additional circadian modulation of the NMDA GluR sensitivity (Colwell 2001; Pennartz et al. 2001). In other neurons, the active regulation of the AMPA GluR plays a major role in determining the contribution of the NMDA GluR to the postsynaptic response (e.g., Durand et al. 1996; Isaac et al. 1995; Luthi et al. 1999). Thus we became interested in better understanding the physiology of AMPA/KA-mediated currents in SCN neurons.

The present study utilized whole cell patch electrophysiological techniques to record AMPA-mediated currents in SCN cells in a brain slice preparation. As a first step, spontaneous excitatory postsynaptic currents (sEPSC) were recorded from SCN slices from animals maintained in a light-dark (LD) cycle. Comparisons were made between ventrolateral (VL) and dorsomedial (DM) regions of the SCN as well as between day and night. Electrophysiological methods were also used to directly measure AMPA-mediated currents in SCN neurons and to determine if the magnitude of these currents varied between SCN regions or from day to night. Next, fluorometric measurements using the Ca^{2+} indicator dye fura2-AM were used to measure AMPA-induced Ca^{2+} transients. Finally, immunocytochemical techniques were used to confirm the presence of AMPA GluR subunits in the SCN and to examine the distribution of the protein throughout the structure.

METHODS

Animals and brain slice preparation

The UCLA Animal Research Committee approved the experimental protocols used in this study. Brain slices were prepared using standard techniques from rats (Sprague-Dawley) between 10 and 14 days of age. For reasons that are not completely understood, infrared differential interference contrast (IR-DIC) videomicroscopy and dye-loading with acetoxymethyl (AM) esters work better in slices from young animals. The circadian oscillator based in the SCN is functional by this age (e.g., Reppert and Schwartz 1984; Shibata and Moore 1987). Rats were killed by decapitation, and brains were dissected and placed in cold oxygenated artificial cerebral spinal fluid (ACSF) containing (in mM) 130 NaCl, 26 NaHCO$_3$, 3 KCl, 5 MgCl$_2$, 1.25 NaH$_2$PO$_4$, 1 CaCl$_2$, and 10 glucose (pH 7.2–7.4; osmolality, 290–300 mosM). After cutting slices, transverse sections (350 μm) were placed in ACSF (25–27°C) for at least 1 h (in this solution, CaCl$_2$ was increased to 2 mM, MgCl$_2$ was decreased to 2 mM). Slices were constantly oxygenated with 95% O$_2$-5% CO$_2$. Slices were placed in a perfusion chamber (Warner Instruments, Hamden, CT) attached to the

stage of the fixed-stage upright microscope. The slice was held down with thin nylon threads glued to a platinum wire and submerged in continuously flowing, oxygenated ACSF at 2 ml/min. Solution exchanges within the slice were achieved by a rapid gravity feed delivery system. In our system, the effects of bath applied drugs begin within 15 s and are typically complete by 1–2 min.

IR-DIC videomicroscopy

Slices were viewed with an upright compound microscope (Olympus BX50), using a water-immersion lens ($\times$40) and DIC optics. They were illuminated with near IR light by placing an IR band-pass filter (750–1050 nm) in the light path. The image was detected with an IR-sensitive video camera (Hamamatsu C2400, Bridgewater, NJ) and displayed on a video monitor. A camera controller allowed analog contrast enhancement and gain control. Cells were typically visualized from 30 to 100 μm below the surface of the slice. In the present study, IR videomicroscopy was utilized to visualize cells within the brain slice and to limit some of the uncertainty as to the cell type. This imaging technique allowed us to clearly see the SCN and to exclude cells from the surrounding hypothalamic regions. In addition, morphological criteria were used to target SCN neurons and to avoid taking measurements from cells that were clearly glia. While size is hardly foolproof, in a few cases, electrophysiological recording and fluorescent imaging were combined to demonstrate that the cells from which Ca^{2+} levels were being measured indeed show the electrical properties of neurons ($n = 5$). Accordingly, it is likely that most of the data were collected from SCN neurons.

Whole cell patch-clamp electrophysiology

Methods were similar to those described previously (Colwell et al. 1998). Briefly, electrodes were pulled on a multistage puller (Sutter P-97, Novato, CA). Electrode resistance in the bath was typically 4–6 MΩ. The standard solution in the patch pipette contains (in mM) 125 Cs-methanesulfonate, 8 HEPES, 5 MgATP, 4 NaCl, 3 KCl, 9 EGTA, MgCl$_2$, 1 GTP, 0.1 leupeptin, and 10 phosphocreatine. The pH was adjusted to 7.25–7.3 using CsOH and the osmolarity to 280–290 mosM using sucrose. For sEPSCs and cell-attached recordings, Cs$^+$ was replaced by K$^+$ in the pipette solution. Whole cell recordings were obtained with an Axon Instruments 200B amplifier and monitored on-line with pCLAMP (Axon Instruments, Foster City, CA). To minimize changes in offset potentials with changing ionic conditions, the ground path used an ACSF agar bridge. Cells were approached with slight positive pressure (2–3 cm H$_2$O), and offset potentials were corrected. The liquid junction potential was measured to be -14 mV. The pipette was lowered to the vicinity of the membrane keeping a positive pressure. After forming a high-resistance seal (2–10 GΩ) by applying negative pressure, a second pulse of negative pressure was used to break the membrane. While entering the whole cell mode, a repetitive test pulse of 10 mV was delivered in a passive potential range (approximately equal to -60 to -70 mV). Whole cell capacitance and electrode resistance were neutralized and compensated (50–80%) using the test pulse. Data acquisition was then initiated. Series and input resistance was monitored repeatedly by checking the response to small pulses in a passive potential range. Series resistance was not compensated, and the maximal voltage error due to this resistance was calculated to be 6 mV. The access resistance of these cells ranged from 20 to 40 MΩ while the cell capacitance was typically between 6 and 18 pF.

Under voltage-clamp ($V_m = -70$ mV), the holding current was monitored throughout the experiment. In addition, the neuron's current-voltage relationship was measured every 2–3 min by moving the cells membrane potential through a series of steps or a ramp of voltages. In these experiments, after the initial control ramps (no drug), each cell was exposed to one concentration of AMPA followed by a wash until the response returned to baseline. The AMPA-evoked

currents were determined from neurons using a ramp command voltage from -70 to $+40$ mV (over 5 s) and then back to -90 mV (1 s). All data were collected from the downward ramp. Current-voltage relationships were calculated as the response to the agonist minus the baseline response in the absence of the agonist. Current measurements were normalized to cell size by dividing peak inward current divided by cell capacitance.

Spontaneous postsynaptic currents were analyzed using the Mini-Analysis program (Synaptosoft, Decatur, GA). The software was used to automatically record the number and peak amplitude of sEPSCs recorded in gap-free mode of pCLAMP software. Each automatically detected event was then manually checked to ensure that the baseline and peak were accurately determined. The mean frequency, amplitude, rise time and decay time of the EPSCs was then calculated for each neuron during 60- to 360-s sampling periods.

Calcium imaging

A cooled CCD camera (Princeton Instruments, Microview model 1317×1035 pixel format) was added to the Olympus fixed-stage microscope to measure fluorescence after passing a dichroic filter with a cutoff at 430 nm. To load the indicator-dye into cells, slices were incubated in membrane permeable fura2-AM (10 μM, Molecular Probes) at 37°C for 10 min. The fluorescence of fura2 was excited alternatively at wavelengths of 357 nm and 380 nm by means of a high-speed wavelength-switching device (Sutter, Lambda DG-4). Image analysis software (MetaFlour, Universal Imaging) allowed the selection of several "regions of interest" within the field from which measurements are taken. To minimize bleaching, the intensity of excitation light and sampling frequency was kept as low as possible. In these experiments the intensity of excitation light was measured as 18 μW out of the objective and measurements were normally made once every 2 s.

Calibration of Ca^{2+} signals

Free $[Ca^{2+}]$ was calculated from the ratio (R) of fluorescence at 357 and 380 nm, using the following equation: $[Ca^{2+}] = K_d \times Sf \times (R - R_{min})/(R_{max} - R)$ (Grynkiewicz et al. 1985). The K_d was assumed to be 135 nM while values for R_{min} and R_{max} were all determined via calibration methods. Initially an in vitro method was used to make estimate values. With this method, rectangular glass capillaries were filled with a high Ca^{2+} (fura2 + 10 mM Ca^{2+}), a low Ca^{2+} (fura2 + 10 mM EGTA) and a control solution without fura2. The fluorescence (**F**) at 380 nm excitation of the low Ca^{2+} solution was imaged and the exposure of the camera adjusted to maximize the signal. These camera settings were then fixed and measurements were made with 380- and 357-nm excitation of the three solutions. $R_{min} =$ F357 in low $Ca^{2+}/$F380 in low Ca^{2+}; $R_{max} =$ F357 in high $Ca^{2+}/$F380 in high Ca^{2+}; Sf = F380 in low $Ca^{2+}/$F380 in high Ca^{2+}. In addition, an in vivo calibration method was also used. For this, SCN cells were loaded via the patch pipette using solutions inside the electrode similar to the normal internal solution but containing either no Ca^{2+} (20 mM EGTA) or 10 mM Ca^{2+} for R_{min} and R_{max}, respectively.

Immunocytochemistry

Animals were anesthetized then perfused transcardially with saline followed by 4% paraformaldehyde. Brains were immersed in fixative overnight and then sectioned (30 μm thick) on a cryostat. Sections were blocked for endogenous peroxidase in 3% hydrogen peroxide plus 10% methanol in PBS. The tissue was then incubated in a serum block solution of 3% normal goat serum and 0.3% Triton X in PBS for 1 h. Sections were incubated with the primary antibody (diluted with serum block solution) for 48 h at 4°C. The tissue was then incubated for 1 h in biotinylated secondary antibody (1:200; diluted with 1% normal goat serum in PBS) at room temperature, followed by incu-

bation in an avidin-biotin-peroxidase (1:50) complex at room temperature for 1 h at room temperature (Vector, Elite kit, Burlingame, CA). Sections were incubated in DAB (final dilution 0.05%) plus hydrogen peroxide (final dilution 0.0015%) in PB for 5–10 min. All previous steps (except serum block) were followed by rinses in PBS (3×5 min each). The tissue was mounted on slides, dehydrated, and cleared in alcohols and xylenes before cover-slipping. Polyclonal antibodies for GluR1 and GluR2/3 raised in rabbit were purchased (Chemicon, Temecula, CA). A dilution series was performed for both antibodies in tissue from 21-day-old animals with optimal dilution found to be 1:100.

Lighting conditions

To investigate possible diurnal variations in any of the measured values, animals were maintained on a daily light-dark cycle consisting of 12 h of light followed by 12 h of dark. It is already well established that cells in the SCN continue to show circadian oscillations when isolated from the animal in a brain slice preparation (e.g., Green and Gillette 1982). Accordingly, care must be taken as to the time in the daily cycle when the data are collected. Some of the animals were killed 30 min before the time that the lights would have turned off in the light-dark (LD) cycle. The data from these animals were collected between zeitgeber time (ZT) 14 and 18 and pooled to form a "night" group. For comparison, some of the animals were killed immediately after the lights came on. The data from these animals were collected between ZT 2–6 and pooled to form a "day" group.

Statistical analyses

Between group differences were evaluated using t-tests or Mann-Whitney rank sum tests when appropriate. Values were considered significantly different if $P < 0.05$. All tests were performed using SigmaStat (SPSS, Chicago, IL). In the text, values are shown as means $\pm$ SE.

RESULTS

Data were collected from a total of 1,272 cells from 104 animals. Every experimental and control group in this study contains data from at least four animals. Each of these cells were determined to be within the SCN by directly visualizing the cell's location with IR-DIC videomicroscopy before any data were collected. In most cases, the IR-DIC video images were sufficient to label a cell as being in VL or DM regions of the SCN. In addition, some neurons were filled with biocytin through the patch electrode and histologically processed. Slices containing these labeled cells were counter-stained with a Nissl stain to confirm the neuron's location within the SCN. All of the cells, which had been visually determined to be in the dorsal (6/6) or ventral (6/6) regions of the SCN, also demonstrated this localization with biocytin fills and Nissl stain.

sEPSCs recorded in VL and DM SCN

The mean frequency and the mean amplitude of sEPSCs recorded at a holding potential of -70 mV were 0.26 ± 0.04 (SE) events/s ($n = 51$; range: 1.29–0.01 events/s) and -17.5 ± 0.8 pA (range: 37–7 pA), respectively. The time to rise and the time to decay (latency of the inward current peak from the baseline) were 1.5 ± 0.04 ms (range: 3.6–1.4 ms) and 2.2 ± 0.1 ms (range: 4.6–1 ms), respectively. These sEPSCs did not appear to be driven by action potentials as neither the amplitude nor the frequency of the currents was significantly altered by the application of the sodium (Na^+) channel blocker

tetrodotoxin (TTX, $n = 6$). The sEPSCs were completely abolished with AMPA/KA GluR antagonist 6-cyano-7-nitro-quinoxaline-2,3-dione (CNQX, 25 μM, 5 of 5 neurons tested), indicating that they are mediated by AMPA/KA GluRs (Fig. 1, *top*). Interestingly, these sEPSCs could be recorded from both VL and DM SCN, and there were no significant differences

between the currents recorded in each region. In the DM SCN, the mean frequency and amplitude of sEPSCs were 0.30 ± 0.07 events/s and −18.9 ± 1.4 pA ($n = 23$), respectively. Whereas in VL SCN, the mean frequency and amplitude of sEPSCs were 0.23 ± 0.03 events/s and −16.3 ± 1.0 pA ($n = 28$), respectively. Thus sEPSCs are not restricted to the retinal recipient VL region but instead are a general feature of cells within the SCN.

Spontaneous EPSCs frequency and amplitude did not vary between day and night in the SCN

The next experiment was designed to determine whether sEPSCs recorded in SCN neurons varied between day and night. These experiments were performed with brain slices taken from animals during their day and compared with data obtained from brain slices from animals during their night. Rats were killed 2–3 h after lights-on for the "day" group or immediately before lights-off for the "night" group. Other than the time that the animals are killed, all conditions between the day and night groups remained constant. The data were collected between zeitgeber time (ZT) 4–8 and ZT 14–16 and were pooled to form "day" and "night" groups, respectively. There were no significant differences in the amplitude, frequency, rise, or fall times of the sEPSCs (Fig. 1). During the day, sEPSCs had a mean amplitude of 16.5 ± 1.0 pA with a mean frequency of 0.27 ± 0.05 Hz (range: 1.2–0.05 Hz; n = 29). Similarly, during the night, the mean amplitude of the sEPSCs was found to be 18.8 ± 1.3 pA with a frequency of 0.25 ± 0.06 Hz (range: 0.65–0.01 Hz; $n = 22$). These data indicate that the presynaptic release as well as postsynaptic sensitivity to glutamate is fairly constant throughout the daily cycle.

AMPA-evoked currents recorded in SCN neurons

Whole cell patch-clamp recording techniques were used to directly measure currents evoked by a submaximal dose of AMPA (25 μM) in SCN neurons. In these experiments, the current required to hold the cell's membrane potential at −70 mV was monitored. In addition, the voltage dependence of the AMPA-evoked currents was measured by moving the cell through either a ramp of voltages (from −70 to 40 then back to −90 mV) or a series of voltage-steps (from −120 to 40 mV) before, during, and after treatment with AMPA in the bath. Because activation of voltage-dependent Na$^+$, Ca^{2+}, and K$^+$ currents could distort measurement of AMPA-evoked currents, cesium (Cs$^+$, 125 mM) was used in the patch pipette while tetraethyl-ammonium chloride (TEA, 10 mM), cadmium (Cd^{2+}, 25 μM), and TTX (1 μM) were in the bath. Figure 2, *top,* shows the current-voltage relationship of an AMPA current recorded using this protocol. Most SCN neurons (91%; 78 of 86 neurons tested) exhibited AMPA-evoked currents. These inward currents exhibited a linear voltage dependency with reversal potentials around 0 mV. AMPA-evoked currents were eliminated by the addition of the AMPA/KA GluR antagonist CNQX (25 μM; $n = 16$).

AMPA-evoked currents could be recorded from both VL and DM SCN, and there were no significant differences between the currents recorded in each region. In the DM SCN, the bath application of AMPA (25 μM) produced a normalized

FIG. 1. Example of spontaneous excitatory postsynaptic currents (sEPSCs) recorded in the day (*top*) in the suprachiasmatic nucleus (SCN). The sEPSCs were blocked by the bath application of CNQX (25 μM; *middle*). The sEPSCs were completely abolished with 6-cyano-7-nitroquinoxalene-2,3-dione (CNQX, 25 μM, 5 of 5 neurons tested), indicating that they are mediated by AMPA/kainate (KA) glutamate receptors (GluRs). Averaged sEPSCs are shown at an expanded time scale as indicated. Experiments were carried out in presence of bicuculline to prevent GABA$_A$-mediated inhibitory postsynaptic currents (IPSCs). *Middle*: histograms indicate the average sEPSC amplitude and frequency recorded in slices from the animal's day ($n = 29$) or night ($n = 22$). The amplitude and frequency did not vary between day and night. *Bottom*: sEPSC frequency as a function of time-of-day (ZT) the recordings were obtained. Although there was a trend for the frequency to be lower at night, this trend was not significant.

FIG. 2. AMPA currents in SCN neurons. Whole cell patch-clamp recording techniques were used to directly measure currents evoked by AMPA in SCN neurons. The voltage dependence of the AMPA-evoked currents was measured by moving the membrane potential of the cell through a series of voltage steps before, during, and after treatment with AMPA (25 μM) in the bath. These experiments were performed in the presence of cadmium (Cd^{2+}, 25 μM), and TTX (1 μM) in the bath. *Top*: an AMPA response recorded using this protocol. AMPA currents blocked by the application of CNQX. *Bottom*: histograms summarizing AMPA evoked currents in the SCN. These currents did not vary between day ($n = 88$) and night ($n = 34$) and were blocked by CNQX ($n = 16$). There was no difference in the magnitude of the AMPA evoked currents recorded in the dorsomedial (DM, $n = 66$) and ventrolateral (VL, $n = 16$) SCN regions.

peak current of -4.1 ± 0.5 pA/pF (range: 0.5 to -21.6 pA/pF; $n = 66$) while in the VL SCN the same treatment produced a peak current of -3.2 ± 0.7 pA/pF (range: 1.2 to -9.9 pA/pF; $n = 16$). The next experiment was designed to determine whether these inward currents evoked by bath application of AMPA varied between day and night in SCN neurons. As described in the preceding text, these experiments were performed with brain slices taken from animals during their day and compared with data obtained from brain slices from animals during their night. Under these conditions, there was no day/night difference in AMPA-evoked inward currents. During the day, AMPA (25 μM, 120–300 s) produced an average peak inward current of -3.7 ± 0.5 pA/pF (range: 0.8 to -16.2 pA/pF; $n = 52$), whereas during the night, this same treatment produced an average peak current of -3.6 ± 0.6 pA/pF (0.3 to -14.8 pA/pF; $n = 33$). These data provide additional support for the conclusions that AMPA-sensitive neurons are found

throughout the SCN and that the sensitivity of these cells to AMPA stimulation does not vary with time of day.

AMPA regulation of Ca^{2+} transients in SCN neurons

A bulk loading procedure was used to load cells with a membrane-permeable form of the Ca^{2+} indicator dye fura2. This procedure loads many cells in SCN slices from young animals (10- to 15-day-old rats were used in the current study). Cells that exhibited uneven loading due to dye sequestration were not included in the data set. Small cell types including glia were easily identified and were not included in the data set. Bath application of AMPA (1–100 μM, 60 s, day) caused Ca^{2+} transients in SCN cells in the brain slice (Fig. 3). For example, AMPA (25 μM, 60 s) produced an average increase in Ca^{2+} of $45 \pm 1\%$ or increased estimated free $[Ca^{2+}]_i$ 20.6 ± 2 nM (range 144 to -12 nM; $n = 1027$). This response was widespread within the SCN with 93% of cells (960/1027) examined showing a Ca^{2+} increase of 5% or greater. AMPA-evoked Ca^{2+} transients could be recorded from both VL and DM SCN, and there were no significant differences between the responses recorded in each region. In the DM SCN, the bath application of AMPA (25 μM) produced a peak Ca^{2+} increase of $43 \pm 3\%$ (mean: 20 ± 1 nM; range: 161 to -3 nM; $n = 300$). In the VL SCN, the same treatment produced a peak Ca^{2+} increase of $47 \pm 5\%$ (mean: 21 ± 2 nM; range: 125 to -0.5 nM; $n = 139$). These AMPA-induced Ca^{2+} transients were blocked by treatment with the AMPA/KA GluR antagonist CNQX (AMPA + CNQX: $1.3 \pm 0.2\%$, $n = 50$).

Neuronal Ca^{2+} influx can be mediated directly by Ca^{2+}-permeable AMPA receptors and indirectly by depolarization-induced activation of voltage-gated Ca^{2+} channels. In addition, in some preparations, reverse Na^+/Ca^{2+} exchange contributes to glutamate-induced Ca^{2+} influx (e.g., Hoyt et al. 1997; Schroeder et al. 1999). To investigate the extracellular source of Ca^{2+} influx, we examined the effect of blocking voltage-gated Ca^{2+} channels with Cd^{2+} and the reverse mode of the Na^+/Ca^{2+} exchange with the selective inhibitor 2-[2-[4-(4-nitrobenzyloxy)phenyl]ethyl]isothiourea (KB-R7943) on the AMPA-induced Ca^{2+} transients. By itself, KB-R7943 (10–25 μM) did not have any effect on resting Ca^{2+} ($0.9 \pm 0.4\%$). When AMPA was applied in the presence of KB-R7943, there was no significant effect on the magnitude of the AMPA-induced Ca^{2+} transients. For example, AMPA (25 μM) in the presence of KB-R7943 increased estimated free $[Ca^{2+}]_i$ by 29.9 nM (range: 168 to -7 nM, $n = 88$), whereas the same cells treated with AMPA alone increased Ca^{2+} by 28.9 nM (range: 155 to -10 nM, $n = 88$). In contrast, the application of the Ca^{2+} channel blocker Cd^{2+} (25 μM) produced a major reduction in the magnitude of the AMPA-evoked response (AMPA alone: $45 \pm 1\%$, $n = 1027$; Cd^{2+} + AMPA: $4 \pm 1\%$, $n = 119$; Fig. 3). In the presence of Cd^{2+}, bath application of AMPA (25 μM) still produced significant Ca^{2+} transients ($P < 0.05$). However, these responses were restricted to only a few cells (10 of 119 SCN cells exhibited a more than 5% increase in Ca^{2+}) with most SCN neurons not exhibiting a detectable Ca^{2+} transient in the presence of Cd^{2+}. Overall, the majority of the AMPA-induced Ca^{2+} influx is sensitive to Cd^{2+}, and it can be assumed to result from the activation of voltage-sensitive Ca^{2+} channels by AMPA.

day ($P < 0.001$; Fig. 4). During the day, bath application of AMPA (25 μM) produced Ca^{2+} transients with an average peak value 31 $\pm$ 26% above baseline having increased estimated $[Ca^{2+}]_i$ 14 $\pm$ 0.7 nM (range: 78 to -12 nM; $n = 418$). The same treatment during the night, caused an average increase of 55 $\pm$ 2% having increased estimated $[Ca^{2+}]_i$ 25 $\pm$ 0.8 nM (range: 144 to -1 nM; $n = 609$). An examination of the distribution of the Ca^{2+} transients (Fig. 4, *bottom*) indicates that the larger mean responses at night was due to a combination of more cells responding to AMPA as well as a larger average response per cell. For example, if analysis is limited to those cells that showed at least a 10% increase in Ca^{2+}, only about half of the cells tested (212/419) reached this threshold compared with 80% at night (473/609). In these responding cells, a diurnal rhythm is still present with AMPA causing an average of 40% change during the day and a 61% change at night. In contrast, treatment with a solution high in potassium (K^+, 50 mM, 15 s) produced Ca^{2+} transients that were not different from day to night (day: 101 $\pm$ 7 nM increase, $n = 83$; night: 102 $\pm$ 6 nM increase, $n = 83$).

FIG. 3. Examples of Ca^{2+} transients measured from SCN cells in a brain slice loaded with the Ca^{2+} indicator dye fura2. *Top*: SCN cells show an increase in Ca^{2+} concentration in response to bath application of AMPA (25 μM, 60 s). Each line represents data collected from an individual cell. These data were collected in the presence of TTX that was included to block voltage-sensitive Na^+ currents. *Middle*: AMPA-induced Ca^{2+} transients were inhibited by the presence of the AMPA/KA GluR antagonist CNQX (25 μM). Data collected from single SCN slice from a 14-day-old rat. *Bottom*: histograms summarizing AMPA regulation of Ca^{2+} levels in the SCN. Bath application of AMPA (25 μM, 60 s) produced Ca^{2+} transients in most cells (93%) within the SCN ($P < 0.001$, $n = 1027$). These AMPA-induced Ca^{2+} transients were blocked by treatment with the AMPA/KA GluR antagonist CNQX (25 μM, $P < 0.001$, $n = 50$) and by treatment with a blocker of high-voltage activating calcium channels (Cd^{2+}, $P < 0.001$, $n = 119$). Finally, there was no difference in the magnitude of the AMPA responses recorded in the DM and VL SCN regions.

Circadian rhythm in the magnitude of AMPA-induced Ca^{2+} transients

The next experiment was designed to determine whether Ca^{2+} transients evoked by bath application of AMPA in SCN neurons varied between day and night. As described in the preceding text, these experiments were performed with brain slices taken from animals during their day and compared with data obtained from brain slices from animals during their night. There was a daily rhythm in Ca^{2+} transients with peak AMPA responses significantly higher during the night than during the

FIG. 4. Diurnal rhythm in AMPA-evoked Ca^{2+} transients in SCN cells. In these experiments, AMPA-evoked Ca^{2+} transients were measured in SCN neurons in brain slices from animals during their day and compared with data obtained from brain slices from animals during their night. Slices were prepared at either ZT 0 for the day group or ZT 11.5 for the night group. Each cell was sampled only once. *Top*: histogram showing average magnitude of AMPA-evoked Ca^{2+} transients measured in SCN neurons in day or night. AMPA-evoked Ca^{2+} transients peaked during night ($P < 0.001$). *Bottom*: distribution of responses in day and night. The larger average Ca^{2+} transients at night was due to a combination of more cells responding to AMPA as well as a larger average response per cell.

Tonic activation of AMPA/KA GluRs may contribute to resting Ca^{2+} concentration and tonic firing rate of some SCN neurons

The next experiment was designed to determine if AMPA-mediated currents tonically influence the firing rate of SCN neurons (Fig. 5, *top*). To address this question, the firing rate of SCN neurons was monitored using the cell-attached recording technique. With this configuration, the patch electrode forms a giga-ohm seal but the membrane is not ruptured. The frequency of spontaneous action potential generation was monitored before and after application of the AMPA/KA GluR antagonist CNQX. Again, CNQX did not have a significant effect ($P > 0.05$) on frequency of firing of the SCN neurons sampled ($n = 16$). However, a subset of SCN neurons (6/16 or 37% of cells examined) did show a marked decrease in firing rate after application of CNQX. These six cells exhibit an average decrease of 49%. To examine the possibility of tonic glutamatergic contribution to the resting Ca^{2+} concentration,
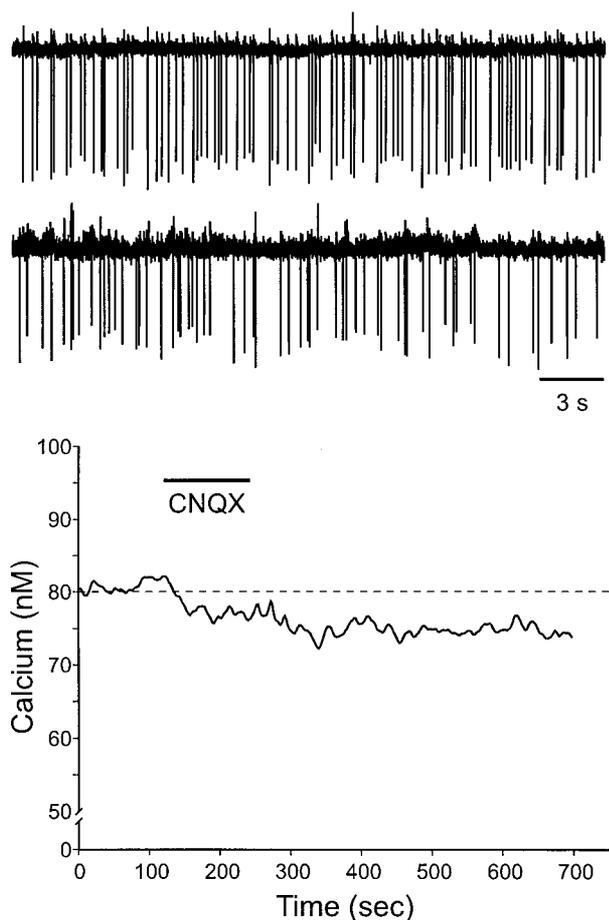
FIG. 5. Application of AMPA/KA GluR antagonist CNQX decreases the firing rate and resting calcium levels of a subset of SCN neurons. *Top*: example of SCN neuron before and after treatment with CNQX (25 μM). The firing rate of this SCN neuron was monitored using the cell-attached recording technique. This treatment with CNQX did not have a significant effect ($P > 0.05$) on frequency of firing of the SCN neurons sampled ($n = 16$). However, as illustrated in this example, a subset of SCN neurons (6/16 or 37% of cells examined) did show a marked decrease in firing rate after application of CNQX. *Bottom*: SCN cell showed a decrease in estimated Ca^{2+} concentration in response to bath application of CNQX (25 μM, 60 s). Overall, there was no significant effect ($P > 0.05$) of CNQX on resting Ca^{2+}; however, many cells (28/73 or 38% of cells examined) did show a reduction of $\geq$5%.

SCN cells were treated with CNQX (25 μM) alone during the day (Fig. 5, *bottom*). Overall, there was no significant effect ($P > 0.05$) of CNQX on resting Ca^{2+} concentration; however, many cells (28/73 or 38% of cells examined) did show a reduction of $\geq$5%. On these cells, application of CNQX produced a modest reduction of 8 ± 0.4%. Together, these results raise the possibility that tonic excitatory drive may influence the activity of at least some cells within the SCN.

AMPA receptors are expressed in SCN in both VL and DM subdivisions

To examine the pattern of expression of receptors likely involved in mediating the AMPA-evoked currents, an antibody raised against an AMPA preferring GluR subunit, GluR1, was utilized (Fig. 6). Rats (age 18–21 days) were perfused at ZT 2–4, and sections containing the SCN were examined immunohistochemically. The GluR1 immunoreactivity was clear in the SCN but more diffuse compared with staining in cortex or hippocampus. Most cell bodies were not clearly stained and those that were stained showed "halo" of immunoreactivity around the soma that may represent staining of cell membrane but not cytoplasm. Staining was most robust in two regions of the SCN including the ventral lateral portions as well as a dorsal region of SCN near the 3rd ventricle. This dorsal region contained the most labeled cell bodies, whereas the staining in the ventral region was mostly limited to the neuropil. There was a core region in the center of the SCN that did not exhibit any clear staining. This general pattern was seen throughout the rostral to caudal extent of the SCN. To look for possible day-night differences in immunoreactivity, staining in tissue collected from ZT 2–4 was compared with those collected between ZT 13–15. Qualitatively, there were no obvious differences between these two time points.

An antibody raised against other AMPA preferring GluR subunits, GluR2/3, was also used (Fig. 6). The GluR2/3 immunolabeling in the SCN was quite different that the GluR1. In general GluR2/3 immunoreactivity was seen on cell bodies and in the neuropil throughout the SCN. The staining was most robust in the ventral region of the SCN near the optic chiasm. This was particularly true in the more rostral regions of the SCN as the staining became more diffuse in the caudal regions. Similar to the GluR1 immunoreactivity, most cell bodies stained showed "halo" of immunoreactivity around the soma. Qualitatively, the staining in tissue collected from ZT 2–4 was similar to that observed from tissue collected between ZT 13–15. Overall, the immunocytochemistry analysis clearly indicates the presence of AMPA preferring GluR subunits within the SCN. These receptors are rather broadly expressed and certainly not restricted to the retino-recipient ventral SCN regions.

DISCUSSION

Summary

In the present study, whole cell patch-clamp techniques were used to measure sEPSCs from SCN neurons. These currents were widespread in the SCN and not just restricted to the retino-recipient region. The sEPSC frequency and amplitude did not vary with the daily cycle. Similarly, currents evoked by the exogenous application of AMPA onto SCN neurons were
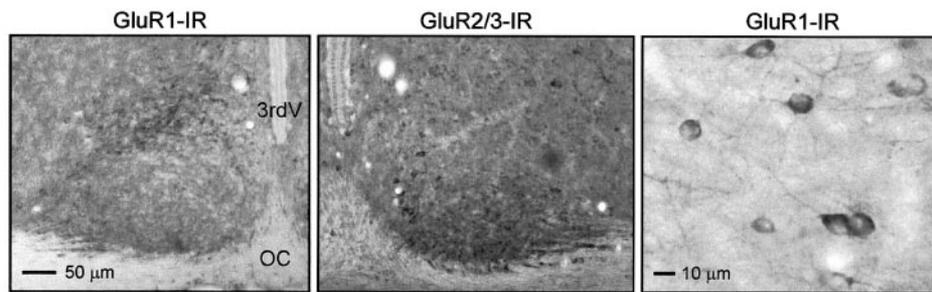
PFIG. 6. Photomicrographs showing immunoreactivity for GluR1 and GluR2/3 in the suprachiasmatic nucleus. 3rdV, third ventricle; OC, optic chiasm. Left panel: The GluR1 immunoreactivity was most robust in 2 regions of the SCN including the ventral lateral portions as well as a dorsal region of SCN near the 3rd ventricle. This dorsal region contained the most labeled cell bodies, whereas the staining in the ventral region was mostly limited to the neuropil. There was a core region in the center of the SCN that did not exhibit any clear staining. This general pattern was seen throughout the rostral to caudal extent of the SCN. Middle panel: GluR2/3 immunoreactivity was seen on cell bodies and in the neuropil throughout the SCN. The staining was most robust in the ventral region of the SCN near the optic chiasm. This was particularly true in the more rostral regions of the SCN as the staining became more diffuse in the caudal regions. Right panel: Higher power view of GluR1-IR. Most cell bodies were not clearly stained and those that were stained showed "halo" of immunoreactivity around the soma that may represent staining of cell membrane but not cytoplasm. Tissue collected from rats (age 18–21 days) that were perfused between ZT 4–6.

widespread within the SCN and did not exhibit a diurnal rhythm in their magnitude. Imaging techniques and the indicator dye fura2 were utilized to estimate AMPA-induced Ca^{2+} changes in SCN cells. The resulting data indicate that AMPA-evoked Ca^{2+} transients were widespread in the SCN and that there was a daily rhythm in the magnitude of AMPA-induced Ca^{2+} transients that peaked during the night. By itself, blocking AMPA/KA GluRs with CNQX decreased the spontaneous firing rate and resting Ca^{2+} of some SCN neurons, suggesting that tonic glutamatergic excitation may influence electrical activity of at least a subset of SCN neurons. Finally, immunohistochemical techniques were used to demonstrate the expression of the AMPA-preferring GluR subunits GluR1 and GluR2/3 within the SCN. Overall, our data demonstrate that glutamatergic synaptic transmission mediated by AMPA/KA GluRs is a general feature of SCN neurons. AMPA-evoked Ca^{2+} responses recorded in SCN neurons expressed a diurnal rhythm, presumably regulated by the circadian timing loop. These observations, coupled with those of previous studies, suggest that glutamatergic synaptic transmission plays an important role in synaptic circuitry throughout the SCN.

Spontaneous EPSCs and AMPA-evoked responses are widespread within the SCN

Anatomical studies support the subdivision of the rat SCN into at least two subdivisions (Moore and Silver 1998; van den Pol 1980). There is a dorsomedial division, or shell, with small cells (10–12 μm in diameter) that typically express vasopressin (VP). These cells are tightly packed with cell bodies in close contact with their neighbors (somato-somatic appositions). This region receives inputs mainly from the cortex, basal forebrain, and other hypothalamic regions while sending projections that largely target the dorsomedial hypothalamus (DMH) and medial subparaventricular zone (sPVZ) (Leak et al. 1999; Moga and Moore 1997). The shell sits atop a ventrolateral division, or core, which contains cells expressing vasoactive intestinal peptide (VIP) or gastrin releasing peptide (GRP). These neurons (12–15 μm in diameter) are found at a lower density, and their cell bodies are in close contact with glia. Both retinal and thalamic input as well as serotonergic

inputs from the raphe mainly project to cells in the core. Neurons from this region project predominantly to the lateral sPVZ. Given that the RHT input to the SCN is known to be glutamatergic and these retinal afferents project to the VIP-containing ventrolateral regions (Card et al. 1981; Tanaka et al. 1993; van den Pol and Tsujimoto 1985), we expected to see a more robust AMPA currents in the retino-recipient, ventrolateral region of the SCN. However, contrary to our expectations, most cells in the SCN show an excitatory response to AMPA in the presence of TTX. For example, in the presented electrophysiological measurements, 91% of cells sampled exhibited an AMPA-induced inward current and 51% expressed sEPSCs. Similarly, ≤93% of fura2-loaded cells showed a Ca^{2+} increase in response to bath application of AMPA. Although peptide expression was not characterized in these cells, video microscopy was used to visually place neurons within general regions of the SCN. Of 86 cells from which AMPA currents were recorded, 66 cells were visually judged to be in the DM SCN and 16 in the VL SCN regions (a few could not be categorized). There were no significant differences between the currents recorded from one region or the other, and certainly SCN neurons in both the VL and DM subdivisions respond to AMPA. Similar observations were made with regard to sEPSPs and AMPA-evoked Ca^{2+} transients (see RESULTS). This physiological data indicating that most cells within the SCN are capable of being excited by AMPA is consistent with our immunocytochemical data suggesting that AMPA preferring GluRs are widely distributed within this nucleus (also see Gannon and Rea 1993, 1994; Mikkelsen et al. 1995; Stamp et al. 1997; van den Pol et al. 1994).

As described previously, the best-known glutamatergic afferents to the SCN are the terminals of the retinal ganglion cells that make up the RHT. These excitatory inputs are restricted to the VL-SCN. The presented data indicate that sEPSCs and AMPA-evoked responses were a general feature of SCN neurons including those in the DM-SCN. This raises an obvious question as to what is the source of these glutamatergic terminals. Retrograde axonal transport of the select neuronal tracer [3H]-aspartate was used to demonstrate possible sources of excitatory input to the SCN in the albino rat (Moga and Moore 1997). Following injection of [3H]-aspartate into the SCN,

neurons were retrogradely labeled in the infralimbic cortex, the lateral septal nucleus, the paraventricular thalamic nucleus, and a variety of hypothalamic nuclei. So besides the retina, it appears that there may be a number of regions that send excitatory projections to the SCN. In addition, though anatomical not well characterized, there is a growing body of evidence that suggests that there are glutamatergic cells within the SCN. The best evidence comes from studies of the pathways by which SCN neurons regulate other hypothalamic nuclei. Stimulation of the SCN evokes short-latency inhibition and excitation of neurons in the ventromedial preoptic area (Sun et al. 2000), the paraventricular nucleus (Cui et al. 2001; also see Csáki et al. 2000), and the arcuate nucleus (Saeb-Parsy et al. 2000). Many of these evoked responses to SCN stimulation had short latencies (<20 ms) and were sensitive to GluR blockers, suggesting that they were mediated by monosynaptic, excitatory connections. As with any of this type of study, it is difficult to rule out that the electrical stimulation activated fibers traveling through the SCN region and not originating in this nucleus. Nevertheless, this body of work certainly suggests that glutamatergic projection neurons may be present within the SCN. Such neurons could easily be involved in communication between SCN regions and be the source of some of the glutamatergic input that we observed throughout the SCN.

Diurnal rhythm in AMPA-evoked calcium transients

The Ca^{2+} influx associated with ligand-gated receptor activation is thought to produce a brief, high-concentration (>100 μM), localized gradients of Ca^{2+} near open channels (e.g., Neher 1998; Yuste et al. 2000). These gradients are rapidly dissipated by diffusion and binding to buffers and would not be seen by slow, volume-averaged measurements used in the present study. However, these rapid influxes would contribute to the Ca^{2+} load in a slower and diffuse Ca^{2+} pool that is referred to as residual Ca^{2+} (e.g., Tank et al. 1995). It is this pool that we measured with the high-affinity Ca^{2+} indicator fura2. These responses are both slower and of lower amplitude than those directly associated with the direct opening of a Ca^{2+} permeable ion channel. It may well be that this Ca^{2+} pool in the soma is more directly related to the role of Ca^{2+} as a regulator of gene expression than the faster transients recorded from the dendrites. The free $[Ca^{2+}]_i$ in the cytoplasm results from the highly regulated balance between the rates of Ca^{2+} influx and removal/buffering. Although the present study did not explore the possibility of circadian regulation of Ca^{2+} removal/buffering mechanisms, there is good reason to suspect that the rhythm in AMPA-induced increases in Ca^{2+} concentration can be accounted for by a daily rhythm in evoked Ca^{2+} influx. Our experimental data indicate that voltage-gated currents are the main contributors to the Ca^{2+} transients (see Fig. 3). AMPA application during the night increased Ca^{2+} levels by 55%, whereas in the presence of Ca^{2+} channel blocker Cd^{2+}, the same treatment increased Ca^{2+} by 4%. This suggests that the Cd^{2+}-sensitive currents are responsible for the vast majority of the AMPA-evoked Ca^{2+} transients. Nevertheless, when these currents were blocked with Cd^{2+}, there were still some cells in which an AMPA-evoked Ca^{2+} transient was present. AMPA GluRs that lack the GluR2 subunit are capable of directly fluxing Ca^{2+} (e.g., Geiger et al. 1995; Hollmann et al. 1991). Two observations from our data suggest that these

Ca^{2+} permeable AMPA receptor types may be present in the SCN. First, immunocytochemical analysis indicated that there was a clear mismatch between expression patterns of GluR1 and GluR2/3. This suggests that some AMPA GluRs may be constructed without the GluR2 subunit especially in the dorsal SCN region. We did not observe any significant regional variation in current density. However, the loss of the GluR2 subunit could have opposing effects on the AMPA-evoked current density. The absence of GluR2 should decrease the AMPA-evoked current at resting membrane potentials (Washburn et al. 1997), whereas single-channel conductance can be dramatically increased by the absence of GluR2 (Swanson et al. 1997). The balance of these opposing effects determines the overall effect changes in GluR2 abundance on GluR properties. Second, though most SCN neurons did not exhibit an AMPA response in the presence of Cd^{2+}, those that did respond (8% of cells tested) exhibited Ca^{2+} transients that were indistinguishable from those measured under normal conditions (28 ± 2 vs. 25 ± 0.8 nM). These cells were located in the DM-SCN and suggest that there may well be a subpopulation of SCN neurons that express Ca^{2+} fluxing AMPA channels.

The simplest mechanistic explanation for the rhythm in Ca^{2+} transients in the SCN is that the rhythm is a direct result of a daily variation in the magnitude of the AMPA-evoked current. However, in this case, data from the present study indicate that AMPA currents do not vary from day to night. There are at least three possible mechanisms that could explain the rhythm. First, the AMPA GluR subunit composition may change from day to night such that the receptor is more permeable to Ca^{2+} during the night. In hippocampal neurons, synaptic activity can lead to the rapid rearrangement of AMPA GluR subunit composition at synapses (Liu and Cull-Candy 2000). Furthermore, in the SCN, a circadian rhythm of AMPA preferring GluR2/3 immunoreactivity has been reported with peak expression during the day (Chambille 1999). This observation is of particular interest because the presence of GluR2 in an AMPA receptor greatly reduces its Ca^{2+} permeability (Geiger et al. 1995: Hollmann et al. 1991). Therefore the higher GluR2/3 immunoreactivity during the day could be reflected in less Ca^{2+}-permeable AMPA GluRs and lower amplitude AMPA-induced Ca^{2+} transients. Second, there is substantial evidence for multiple types of voltage-dependent Ca^{2+} channels in other regions of the CNS. These include low-voltage activating Ca^{2+} channels (LVA) and high-voltage activating Ca^{2+} channels (HVA) that are generally subdivided into L, N, P, R, and Q-types. Although not extensively studied, there is evidence for both HVA and LVA Ca^{2+} currents in SCN neurons (Akasu et al. 1993; Huang 1993). We have found that Cd^{2+} (25 μM) blocks the HVA but not the LVA Ca^{2+} currents in SCN neurons (Colwell unpublished data). Therefore a second possible mechanism that could explain the rhythm in AMPA-evoked response would be a rhythm in HVA Ca^{2+} currents. Other studies have reported evidence for diurnal rhythms in membrane properties of SCN neurons (de Jeu et al. 1998; Jiang et al. 1997; Schaap et al. 1999). Third, it may well be that the rhythm in AMPA evoked responses is due to a regulation of Ca^{2+}-induced release of Ca^{2+} from internal stores. Previous studies have implicated ryanodine receptors and intracellular calcium stores in mediating light and glutamate induced phase delays of the mammalian circadian clock (Ding et al. 1998; Hamada et al. 1999). These three possibil-

ities are not mutually exclusive and can be experimentally resolved.

Functional importance

One of the fundamental features of circadian oscillators is that their response to environmental stimulation varies depending on the phase of the daily cycle when the stimuli are applied. For example, the same light treatment, which can produce phase shifts of the oscillator when applied during the subjective night, has no effect when applied during the subjective day. This periodic sensitivity to photic stimulation is a central feature of entrainment, i.e., the process by which circadian oscillators are synchronized to the environment. Despite its importance, the cellular and molecular mechanisms behind this differential sensitivity are just beginning to be explored in mammals. There is some evidence that this regulation may occur at the level of the SCN neurons. Two previous studies have demonstrated a daily rhythm in the response of SCN cells to photic and electrical stimulation of the RHT (Cui and Dyball 1996; Meijer et al. 1998). In addition, electrical stimulation of the RHT causes the same daily pattern of light-like phase shifts of the circadian system both in vivo (de Vries et al. 1994) and in vitro (Shibata and Moore 1993), i.e., phase shifts during the night but not during the day. Glutamate is the transmitter at the retinal input to the SCN and exogenous application of GluR agonists cause light-like phase shifts of the circadian rhythm in neuronal activity in the SCN in vitro (Ding et al. 1994; Shibata et al. 1994; Shirakawa and Moore 1994). In addition, two recent studies demonstrate that there are daily rhythms in both synaptic evoked, NMDA-induced Ca^{2+} transients and NMDA currents recorded from SCN neurons in a brain slice preparation (Colwell 2001; Pennartz et al. 2001).

In many synapses, AMPA and NMDA GluRs work in concert with the AMPA GluRs that are responsible for the initial depolarization of the postsynaptic membrane. This depolarization is required before the neuron's membrane potential moves into the voltage range at which the NMDA GluR can become activated. A recent study indicates that in the SCN the relative contribution of the NMDA GluR to the postsynaptic response is larger during the night than during the day (Pennartz et al. 2001). The active regulation of AMPA GluR can play a major role in determining the contribution of NMDA GluR to the postsynaptic response. For example, in some synapses, it appears that NMDA GluRs, but not AMPA GluRs are expressed. This makes this connection electrophysiologically "silent" as the postsynaptic cell would not normally be in a voltage range in which the NMDA receptors would be active. However, in response to appropriate patterns of stimulation, the AMPA GluRs can be rapidly inserted into the postsynaptic membrane (e.g., Durand et al. 1996; Isaac et al. 1995; Luthi et al. 1999). We thought that the rapid regulation of AMPA receptors could be a logical mechanism to gate the light input to the circadian system. However, our data do not support such a hypothesis (also see Pennartz et al. 2001).

Even if the current evoked by AMPA GluRs is not gated by the circadian system, these receptors are still likely to play critical role in transduction of environmental information to the SCN. First, we have found that AMPA/KA GluR mediate most excitatory synaptic transmission in the SCN (also see Cahill and Menaker 1989; Cui and Dyball 1996; de Vries et al. 1994;

Jiang et al. 1997; Kim and Dudek 1991) and are a general feature of SCN neurons. Both spontaneous and evoked AMPA/KA-mediated currents were just as prevalent in the DM-SCN as in the VL-SCN. These GluRs are likely to function as permissive partners to the NMDA-evoked response as they are required to depolarize the cell and remove the magnesium blockade of the NMDA GluR. Support for this model of coordination between NMDA and AMPA/KA GluRs comes from studies of light and glutamate regulation of gene expression in the SCN (e.g., Abe et al. 1992; Guido et al. 1999; Schurov et al. 1999). For example, in cultured SCN cells, neither AMPA nor NMDA alone causes much change in CREB phosphorylation while application of the two agonists together caused a robust induction of pCREB immunoreactivity (Schurov et al. 1999). By itself, application of AMPA causes phase shifts of neural activity rhythms recorded from SCN brain slices during the night and prevent 5HT-evoked phase shifts during the day (e.g., Prosser 2001; Shibata et al. 1994). Finally, administration of AMPA/KA GluR blockers (CNQX, DNQX) prevents the effects of light on the circadian rhythm of wheel-running activity (Colwell and Menaker 1992; Rea et al. 1993). These observations lead us to conclude that AMPA/KA receptors are likely to play a broad role in transduction of signals onto the SCN.

REFERENCES

ABE H, RUSAK B, AND ROBERTSON HA. NMDA and non-NMDA antagonists inhibit photic induction of Fos protein in the hamster suprachiasmatic nucleus. Brain Res Bull 28: 831–833, 1992.

AKASU T, SHOJI S, AND HASUO H. Inward rectifier and low-threshold calcium currents contribute to the spontaneous firing mechanism in neurons of the rat suprachiasmatic nucleus. Pflügers Arch 425: 109–116, 1993.

BALSALOBRE A, DAMIOLA F, AND SCHIBLER U. A serum shock induces circadian gene expression in mammalian tissue culture cells. Cell 93: 929–937, 1998.

CAHILL GM AND MENAKER M. Effects of excitatory amino acid receptor antagonists and agonists on suprachiasmatic nucleus responses to retinohypothalamic tract volleys. Brain Res 479: 76–82, 1989.

CARD JP, BRECHA N, KARTEN HJ, AND MOORE RY. Immunocytochemical localization of vasoactive intestinal peptide-containing cells and processes in the suprachiasmatic nucleus of the rat. J Neurosci 1: 1289–1303, 1981.

CHAMBILLE I. Circadian rhythm of AMPA receptor GluR2/3 subunit-immunoreactivity in the suprachiasmatic nuclei of Syrian hamster and effect of a light-dark cycle. Brain Res 833: 27–38, 1999.

COLWELL CS. NMDA-evoked calcium transients and currents in the suprachiasmatic nucleus: gating by the circadian system. Eur J Neurosci 13: 1420–1428, 2001.

COLWELL CS, CEPEDA C, CRAWFORD C, AND LEVINE MS. Postnatal development of NMDA evoked responses in the neostriatum. J Dev Neurobiol 20: 154–163, 1998.

COLWELL CS AND MENAKER M. NMDA as well as non-NMDA receptor antagonists can prevent the phase shifting effects of light on the circadian system of the golden hamster. J Biol Rhythms 7: 125–136, 1992.

COLWELL CS AND MENAKER M. Excitatory Amino Acids: Their Role in Neuroendocrine Function. New York: CRC, 1996, p. 223–252.

CSÁKI A, KOCSIS K, HALÁSZ B, AND KISS J. Localization of glutamatergic/aspartatergic neurons projecting to the hypothalamic paraventricular nucleus studied by retrograde transport of [³H]-aspartate autoradiography. Neuroscience 101: 637–655, 2000.

CUI LN, CODERRE E, AND RENAUD L P. Glutamate and GABA mediate suprachiasmatic nucleus inputs to spinal-projecting paraventricular neurons. Am J Physiol Regulatory Integrative Comp Physiol 281: R1283–1289, 2001.

CUI LN AND DYBALL REJ. Synaptic input from the retina to the suprachiasmatic nucleus changes with the light-dark cycle in the Syrian hamster. J Physiol (Lond) 497: 483–493, 1996.

DE JEU M, HERMES M, AND PENNARTZ C. Circadian modulation of membrane properties in slices of rat suprachiasmatic nucleus. *Neuroreport* 9: 3725–3729, 1998.

DE VRIES MJ, TREEP JA, DE PAUW ESD, AND MEIJER JH. The effects of electrical stimulation of the optic nerves and anterior optic chiasm on the circadian activity rhythm of the Syrian hamster: involvement of excitatory amino acids. *Brain Res* 642: 206–212, 1994.

DING JM, BUCHANAN GF, TISCHKAU SA, CHEN D, KURIASHKINA L, FAIMAN LE, ALSTER JM, MCPHERSON PS, CAMPBELL KP, AND GILLETTE MU. A neuronal ryanodine receptor mediates light-induced phase delays of the circadian clock. *Nature* 394: 381–384, 1998.

DING JM, CHEN D, IBER ET, FAIMAN LE, REA MA, AND GILLETTE MU. Resetting the biological clock: mediation of nocturnal circadian shifts by glutamate and NO. *Science* 266: 1713–1717, 1994.

DURAND GM, KOVALCHUK Y, AND KONNERTH A. Long-term potentiation and functional synapse induction in developing hippocampus. *Nature* 381: 71–75, 1996.

EBLING FJP. The role of glutamate in the photic regulation of the suprachiasmatic nucleus. *Prog Neurobiol* 50: 109–132, 1996.

GANNON RL AND REA MA. Glutamate receptor immunoreactivity in the rat suprachiasmatic nucleus. *Brain Res* 622: 337–342, 1993.

GANNON RL AND REA MA. In situ hybridization of antisence mRNA oligonucleotides for AMPA, NMDA and metabotropic glutamate receptor subtypes in the rat suprachiasmatic nucleus at different phases of the circadian cycle. *Mol Brain Res* 23: 338–344, 1994.

GEIGER JR, MELCHER T, KOH DS, SAKMANN B, SEEBURG PH, JONAS P, AND MONYER H. Relative abundance of subunit mRNAs determines gating and Ca^{2+} permeability of AMPA receptors in principal neurons and interneurons in rat CNS. *Neuron* 15: 193–204, 1995.

GILLETTE MU. Cellular and biochemical mechanisms underlying circadian rhythms in vertebrates. *Curr Opin Neurobiol* 7: 797–804, 1997.

GREEN DJ AND GILLETTE R. Circadian rhythm of firing rate recorded from single cells in the rat suprachiasmatic brain slice. *Brain Res* 245: 198–200, 1982.

GRYNKIEWICZ G, POENIE M, AND TSIEN RY. A new generation of Ca^{2+} indicators with greatly improved fluorescence properties. *J Biol Chem* 260: 3440–3450, 1985.

GUIDO ME, DE GUIDO L, GOGUEN D, ROBERTSON HA, AND RUSAK B. Differential effects of glutamatergic blockade on circadian and photic regulation of gene expression in the hamster suprachiasmatic nucleus. *Mol Brain Res* 67: 247–257, 1999.

HAMADA T, LIOU SY, FUKUSHIMA T, MARUYAMA T, WATANABE S, MIKOSHIBA K, AND ISHIDA N. The role of inositol trisphosphate-induced Ca^{2+} release from IP_3-receptor in the rat suprachiasmatic nucleus on circadian entrainment mechanism. *Neurosci Lett* 263: 125–128, 1999.

HOLLMANN M, HARTLEY M, AND HEINEMANN S. Ca^{2+} permeability of KA-AMPA-gated glutamate receptor channels depends on subunit composition. *Science* 252: 851–853, 1991.

HOYT KR, ARDEN SR, AIZENMAN E, AND REYNOLDS IJ. Reverse Na^+/Ca^{2+} exchange contributes to glutamate-induced intracellular Ca^{2+} concentration increases in cultured rat forebrain neurons. *Mol Pharmacol* 53: 742–749, 1997.

HUANG R-C. Sodium and calcium currents in acutely dissociated neurons from rat suprachiasmatic nucleus. *J Neurophysiol* 70: 1692–1703, 1993.

IBATA Y, OKAMURA H, TANAKA M, TAMADA Y, HAYASHI S, IIJIMA N, MATSUDA T, MUNEKAWA K, TAKAMATSU T, HISA Y, SHIGEYOSHI Y, AND AMAYA F. Functional morphology of the suprachiasmatic nucleus. *Front Neuroendocrinol* 20: 241–268, 1999.

ISAAC JT, NICOLL RA, AND MALENKA RC. Evidence for silent synapses: implications for the expression of LTP. *Neuron.* 15: 427–434, 1995.

JIANG ZG, YANG YQ, LIU ZP, AND ALLEN CN. Membrane properties and synaptic inputs of suprachiasmatic nucleus neurons in rat brain slices. *J Physiol (Lond)* 499: 1: 141–159, 1997.

KIM YI AND DUDEK FE. Intracellular electrophysiological study of suprachiasmatic nucleus neurons in rodents: excitatory synaptic mechanisms. *J Physiol (Lond)* 444: 269–287, 1991.

KING DP AND TAKAHASHI JS. Molecular genetics of circadian rhythms in mammals. *Annu Rev Neurosci 23* 713–742: 2000.

LEAK RK, CARD JP, AND MOORE RY. Suprachiasmatic pacemaker organization analyzed by viral transynaptic transport. *Brain Res* 819: 23–32, 1999.

LIU SQ AND CULL-CANDY SG. Synaptic activity at calcium-permeable AMPA receptors induces a switch in receptor subtype. *Nature* 405: 454–458, 2000.

LUTHI A, CHITTAJALLU R, DUPRAT F, PALMER MJ, BENKE TA, KIDD FL, HENLEY JM, ISAAC JT, AND COLLINGRIDGE GL. Hippocampal LTD expression involves a pool of AMPARs regulated by the NSF-GluR2 interaction. *Neuron* 24: 389–399, 1999.

MEIJER JH, WATANABE K, SCHAAP J, ALBUS H, AND DETARI L. Light responsiveness of the suprachiasmatic nucleus: long-term multiunit and single-unit recordings in freely moving rats. *J Neurosci* 18: 9078–9087, 1998

MIKKELSEN JD, LARSEN PJ, MICK G, VRANG N, EBLING FJ, MAYWOOD ES, HASTINGS MH, AND MOLLER M. Gating of retinal inputs through the suprachiasmatic nucleus: role of excitatory neurotransmission. *Neurochem Int* 27: 263–272, 1995.

MINTZ EM, MARVEL CL, GILLESPIE CF, PRICE KM, AND ALBERS HE. Activation of NMDA receptors in the suprachiasmatic nucleus produces light-like phase shifts of the circadian clock in vivo. *J Neurosci* 19: 5124–5130, 1999.

MOGA MM AND MOORE RY. Organization of neural inputs to the suprachiasmatic nucleus in the rat. *J Comp Neurol* 389: 508–534, 1997.

MOORE RY. Entrainment pathways and the functional organization of circadian. *Prog Brain Res* 111: 103–119, 1996.

MOORE RY AND SILVER R. Suprachiasmatic nucleus organization. *Chronobiol Int* 15: 475–487, 1998.

MORIN LP. The circadian visual system. *Brain Res Rev* 19: 102–127, 1994.

NEHER E. Vesicle pools and Ca^{2+} microdomains: new tools for understanding their roles in neurotransmitter release. *Neuron* 20: 389–399, 1998.

OBRIETAN K, IMPEY S, AND STORM DR. Light and circadian rhythmicity regulate MAP kinase activation in the suprachiasmatic nuclei. *Nat Neurosci* 1: 693–700, 1998.

PENNARTZ CM, HAMSTRA R, AND GEURTSEN AM. Enhanced NMDA receptor activity in retinal inputs to the rat suprachiasmatic nucleus during the subjective night. *J Physiol (Lond)* 532: 181–194, 2001.

PROSSER RA. Glutamate blocks serotonergic phase advances of the mammalian circadian pacemaker through AMPA and NMDA receptors. *J Neurosci* 21: 7815–7822, 2001.

REA MA, BUCKLEY B, AND LUTTON LM. Local administration of EAA antagonists blocks light-induced phase shifts and c-fos expression in the hamster SCN. *Am J Physiol Regulatory Integrative Comp Physiol* 265: R1191–1198, 1993.

REPPERT SM AND SCHWARTZ WJ. The suprachiasmatic nuclei of the fetal rat: characterization of a functional circadian clock using 2-deoxyglucose. *J Neurosci* 4: 1677–1682, 1984.

REPPERT SM AND WEAVER DR. Molecular analysis of mammalian circadian rhythms. *Annu Rev Physiol* 63: 647–676, 2001.

SAEB-PARSY K, LOMBARDELLI S, KHAN FZ, MCDOWALL K, AU-YONG IT, AND DYBALL RE. Neural connections of hypothalamic neuroendocrine nuclei in the rat. *J Neuroendocrinol* 12: 635–648, 2000.

SCHAAP J, BOS NP, DE JEU MT, GEURTSEN AM, MEIJER JH, AND PENNARTZ CM. Neurons of the rat suprachiasmatic nucleus show a circadian rhythm in membrane properties that is lost during prolonged whole-cell recording. *Brain Res* 815: 154–166, 1999.

SCHROEDER UH, BREDER J, SABELHAUS CF, AND REYMANN KG. The novel Na^+/Ca^{2+} exchange inhibitor KB-R7943 protects CA1 neurons in rat hippocampal slices against hypoxic/hypoglycemic injury. *Neuropharmacology* 38: 319–321, 1999.

SCHUROV IL, MCNULTY S, BEST JD, SLOPER PJ, AND HASTINGS MH. Glutamatergic induction of CREB phosphorylation and Fos expression in primary cultures of the suprachiasmatic hypothalamus in vitro is mediated by coordinate activity of NMDA an

MORIN LP. The circadian visual system. *Brain Res Rev* 19: 102–127, 1994.

SHIBATA S AND MOORE RY. Development of neural activity in the rat suprachiasmatic nucleus. *Brain Res* 431: 311–315, 1987.

SHIBATA S AND MOORE RY. Neuropeptide Y and optic chiasm stimulation affect suprachiasmatic nucleus circadian function in vitro. *Brain Res* 615: 95–100, 1993.

SHIBATA S, WATANABE A, HAMADA T, ONO MAND WATANABE S. *N*-methyl-D-aspartate induces phase shifts in circadian rhythm of neuronal activity of rat SCN in vitro. *Am J Physiol Regulatory Integrative Comp Phyiol.* 267: R360–364, 1994.

SHIRAKAWA T AND MOORE RY. Glutamate shifts the phase of the circadian neuronal firing rhythm in the rat suprachiasmatic nucleus in vitro. *Neurosci Lett* 178: 47–50, 1994.

STAMP JA, PIGGINS HD, RUSAK B, AND SEMBA K. Distribution of ionotropic glutamate receptor subunit immunoreactivity in the suprachiasmatic nucleus and intergeniculate leaflet of the hamster. *Brain Res* 756: 215–224, 1997.

SUN X, RUSAK B, AND SEMBA K. Electrophysiology and pharmacology of projections from the suprachiasmatic nucleus to the ventromedial preoptic area in rat. *Neuroscience* 98: 715–728, 2000.

MORIN LP. The circadian visual system. *Brain Res Rev* 19: 102–127, 1994.

SWANSON GT, KAMBOJ SK, AND CULL-CANDY SG. Single-channel properties of recombinant AMPA receptors depend on RNA editing, splice variation, and subunit composition. *J Neurosci* 17: 58–69, 1997.

TANAKA M, ICHITANI Y, OKAMURA H, TANAKA Y, AND IBATA Y. The direct retinal projection to VIP neuronal elements in the rat SCN. *Brain Res Bull* 31: 637–640, 1993.

TANK DW, REGEHR WG, AND DELANEY KR. A quantitative analysis of presynaptic calcium dynamics that contribute to short-term enhancement. *J Neurosci* 15: 7940–7952, 1995.

VAN DEN POL AN. The hypothalamic suprachiasmatic nucleus of the rat: intrinsic anatomy. *J Comp Neurol* 191: 661–702, 1980.

VAN DEN POL AN, HERMANS-BORGMEYER I, HOFER M, GHOSH P, AND HEINEMANN S. Ionotropic glutamate-receptor gene expression in hypothalamus: localization of AMPA, kainate, and NMDA receptor mRNA with in situ hybridization. *J Comp Neurol* 343: 428–444, 1994.

VAN DEN POL AN AND TSUJIMOTO KL. Neurotransmitters of the hypothalamic suprachiasmatic nucleus: immunocytochemical analysis of 25 neuronal antigens. *Neuroscience* 15: 1049–1086, 1985.

WASHBURN MS, NUMBERGER M, ZHANG S, AND DINGLEDINE R. Differential dependence on GluR2 expression of three characteristic features of AMPA receptors. *J Neurosci* 17: 9393–9406, 1997.

WELSH DK, LOGOTHETIS DE, WEISTER M, AND REPPERT SM. Individual neurons dissociated from rat suprachiasmatic nucleus express independently phase circadian firing patterns. *Neuron* 14: 697–706, 1995.

YUSTE R., MAJEWSKA A, AND HOLTHOFF K. From form to function: calcium compartmentalization in dendritic spines. *Nat Neurosci* 3: 653–659, 2000.